Bow-Tie-Antenna-Coupled Terahertz Detectors using AlGaN/GaN Field-Effect Transistors with 0.25 Micrometer Gate Length

Maris Bauer[1*], Alvydas Lisauskas[1], Sebastian Boppel[1], Martin Mundt[1], Viktor Krozer[1,2], Hartmut G. Roskos[1], Serguei Chevtchenko[2], Joachim Würfl[2], Wolfgang Heinrich[2] and Günther Tränkle[2]
[1] Physikalisches Institut, Johann Wolfgang Goethe Universität, Frankfurt am Main, Germany
[*] m.bauer@physik.uni-frankfurt.de
[2] Ferdinand-Braun-Institut, Leibniz-Institut für Höchstfrequenztechnik (FBH), Berlin, Germany

***Abstract*—We report on the design and characterization of terahertz detection devices using field-effect transistors and on-chip broadband antennas. Experimental results from measurements on high-electron-mobility transistors fabricated with a AlGaN/GaN heterostructure are presented. Physical device parameters are extracted. The measured samples exhibit good noise-equivalent power (NEP) values at 0.6 THz of down to $\sim$ 125 pW/$\sqrt{\text{Hz}}$. The responsivity is maximized by gate width. The best NEP value is found for the narrowest devices.**

***Keywords*—AlGaN/GaN terahertz detectors; high-responsivity devices; antenna-coupled high-electron-mobility transistors; integrated field-effect transistors**

I. Introduction

The development of terahertz (THz) detection devices using distributed self-mixing in field-effect transistors (FETs) is a very active field of scientific research. The underlying concept [1] is a universal one and has been implemented in many material and device systems such as complementary metal-oxide-semiconductor (CMOS) silicon technology [2], [3]. As gallium nitride (GaN) microelectronics continues to develop into an important platform for high-power and high-frequency applications [4], and even offers the option of on-chip fusion of electronic and optical functions, it is highly desirable to provide for a THz detection capability also in this technology [5], [6]. An intriguing option of GaN electronics is its potential for the development of on-chip THz sensor systems exploiting the THz-emission [7] as well as the THz-detection capability of GaN FETs [8], [9].

In this contribution, we present a dual-transistor design for broad-band THz detectors using standard AlGaN/GaN high-electron-mobility transistor (HEMT) technology. We discuss design considerations for optimized THz responsivity and noise-equivalent power (NEP). Special emphasis is laid on the role of the channel width. From the measured response to radiation at 0.6 THz and from the dc transfer characteristics, the mobility, non-ideality factor, and threshold voltage data are derived with a simplified model which is able to describe both the I/V curves and the THz response.

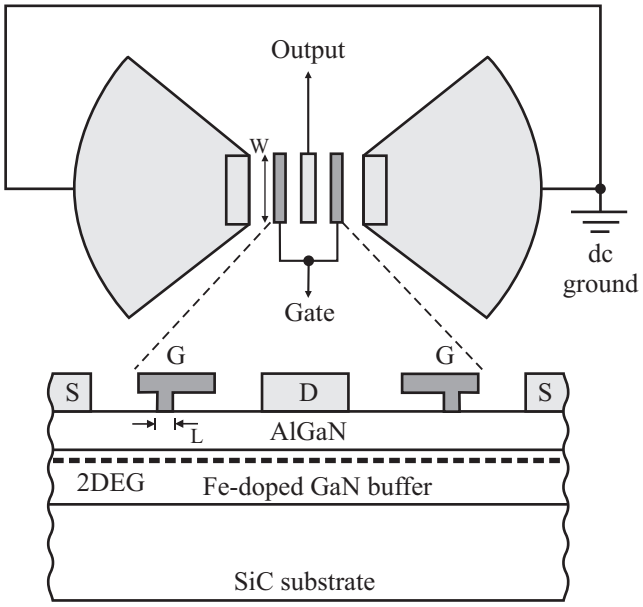

Fig. 1. Schematic of the antenna-coupled GaN HEMT high-frequency design. At the top, the bow-tie antenna with the transistor pair is shown. The source contacts (S) lie on dc ground. The common drain contact (D), which is also used for signal read-out, is placed at the node of the antenna, constituting a virtual ac ground. The bottom scheme shows a cross-sectional view of the device.

II. Theory

Non-resonant THz detection in field-effect transistors is based on distributed self-mixing of radiation-induced (over-)damped plasma wave oscillations [1], [9]–[11]. Since self-mixing is not frequency-limited by the transit time of electronic transport inside the FET channel, rectification of frequencies high above the transistor's cutoff frequency can be observed [11]. In particular, this sensitivity can be exploited to develop THz detection devices working over a large frequency range at room temperature. For a successful detector design, one needs knowledge of all contributions to the high-frequency device impedance arising from the channel, the contacts, etc. In the THz frequency range, the measurement of the parameters

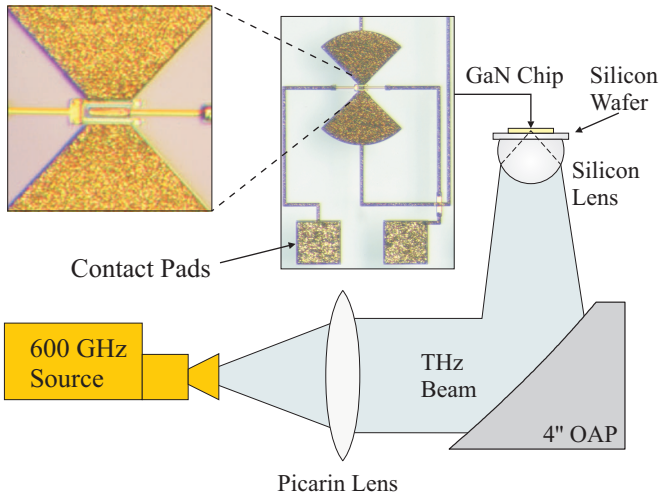

Fig. 2. The experimental setup, which was used to characterize the GaN FET detectors. A collimated 0.6 THz source was focused onto the GaN chip by a 4" OAP and a hyper-hemispherical silicon lens with a diameter of 12 mm. The photographs show magnified images of a single detector with the FET in the center of the on-chip antenna.

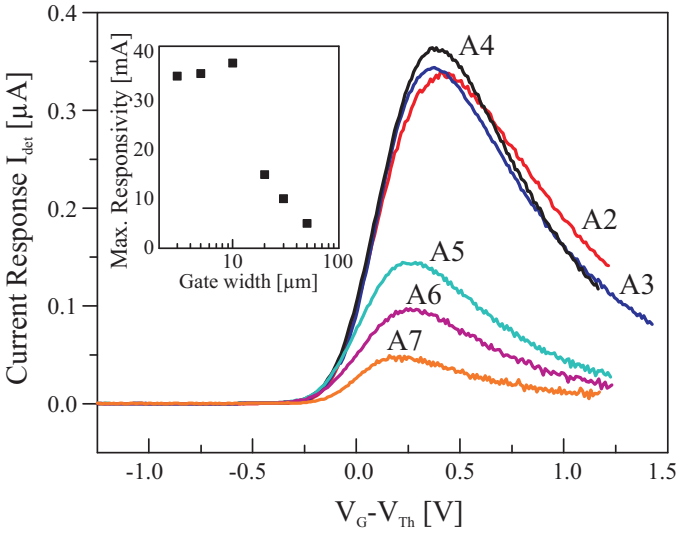

Fig. 3. Measured current response signals I_{det} as read-out by lock-in amplifier. The raw measurement data have been shifted by individual threshold voltages extracted from resistance-curve fits based on (1). The inset shows the maximum current responsivity versus transistor gate width W.

is extremely challenging. Fortunately, the hydrodynamic transport theory [1], which underlies the self-mixing effect, links the THz mixing performance of the FET close to the threshold to its quasi-static transport properties there [11], [12]. This allows - within the limits of the validity of the hydrodynamic approach - to come to a practical way for the determination of the relevant parameters.

A crucial input to the theory is a model for the dependence of the channel's carrier density on gate voltage V_{G}, directly determining the channel resistance R_{d}. Physics-based analytical models have been the subject of investigations, e.g. by Khandelwah et al., describing the relation between the gate capacitance of GaN HEMT devices and the charge density in the transistor's two-dimensional electron gas (2DEG) [13]. However, as has been stated there, a proper choice of fitting parameters in a unified charge control model originally developed by Shur et al. [14] for metal-oxide-semiconductor FETs (MOSFETs) can lead to a satisfactory description of $R_{\mathrm{d}}\,(V_{\mathrm{G}})$:

$$R_{\mathrm{d}} = \frac{L}{\mu\eta V_{\mathrm{T}} C_{\mathrm{G}} W \ln\left(1+\frac{1}{2}\exp\left(\frac{V_{\mathrm{G}}-V_{\mathrm{Th}}}{\eta V_{\mathrm{T}}}\right)\right)} \qquad (1)$$

Here, V_{T} is the thermal voltage, L and W are the gate length and width (compare Fig. 1), respectively, and C_{G} is the gate-to-channel capacitance per unit area. All these parameters are fixed as design parameters for a given transistor. It is found that using the electron mobility μ, the subthreshold ideality factor η and the transistor's threshold voltage V_{Th} as fitting parameters, leads to a good accordance with experimentally obtained resistance data. Note that in this description, only the gated regions of the transistor channel are considered, assuming a constant resistance in the ungated regions. Equation (1) will be used in Section V for the analysis of experimental resistance curves of the GaN HEMTs.

III. Devices

HEMT structures with 0.25 μm gate lengths L and varying gate widths W were fabricated in a AlGaN/GaN process at FBH Berlin [15]. The upper part of Fig. 1 shows a schematic view of the high-frequency design elements, such as the on-chip integrated bow-tie antenna and the transistor's source, gate, and drain contacts. The gates are laid out with field plates. For efficient THz self-mixing, plasma waves have to be launched into the channel from one side only. This is ensured by the chosen symmetric two-transistor layout. The source contacts, which are directly connected to the high-frequency antenna, lie on dc ground, whereas the transistors' common drain contact is placed on virtual ac ground at the antenna node. The rectified THz signal is read out from the device via the drain terminal. In the lower part of Fig. 1, a cross-sectional view of the AlGaN/GaN HEMT is displayed. The heterostructure is grown on semi-insulating silicon carbide (SiC) substrate. Details on the epitaxial growth process and device fabrication can be found in [15], [16]. The transistor channel with the 2DEG is formed at the interface of the GaN buffer layer and the AlGaN layer. The transistor's source, drain, and gate contacts are each connected to 80x80 μm^2 contact pads for probing (compare photograph in Fig. 2). GaN chips with a series of HEMT designs, varying in transistor geometry and bow-tie antenna size, were available at the time of the experiments described below. In all designs, care was taken to minimize the access resistance by keeping the ungated regions of the HEMTs short. The total channel length, i.e., the drain-source distance, amounts to 1.75 μm. The results described in this work are based on a set of six transistors with different gate widths and integrated antennas, optimized for a resonance frequency of 600 GHz. Although antenna designs with higher resonance frequencies were also available, this particular set of detectors was chosen in correspondence to the frequency of the available THz source.

IV. Experimental Setup

An experimental setup for device characterization was realized using an all-electronic source. In detail, a W-band source was driven at 16.385 GHz by an amplitude-modulated

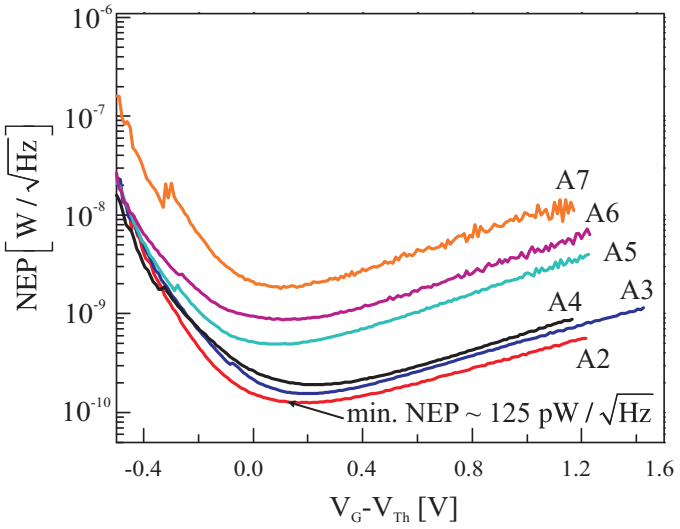

Fig. 4. Device NEPs calculated by (3) from measured current responsivities. A minimum NEP of 125 pW/$\sqrt{\text{Hz}}$ with respect to the total available beam power could be observed.

synthesizer with a modulation frequency of 333 Hz. This frequency served as a reference for lock-in detection. The output of the W-band source is up-converted by a chain of active frequency multipliers, resulting in an effective output frequency of 589.86 GHz. The radiation is emitted via a high-directivity horn antenna, which is optimized for 0.6 THz. Fig. 2 depicts the measurement setup for THz characterization. After the source, the THz beam was collimated using a Picarin lens of 10 cm focal length. An off-axis parabolic mirror (OAP) with a focal length of 4" was used for pre-focusing of the parallel beam. However, in order to achieve optimal focusing onto the small on-chip bow-tie antennas, an aplanatic hyper-hemispherical silicon lens with a diameter of 12 mm and a height of 6.8 mm was employed [17]. The actual sample, i.e., the GaN chip with the various transistor designs, is placed on an additional silicon wafer of 440 μm thickness, which is part of a probe station (not shown in the figure), and which can be moved perpendicular to the optical axis of the setup by micrometer stages. In this way, the different detectors on the chip can be selected to be illuminated by the THz beam. The HEMTs were electrically contacted with the help of micromanipulator probes, which were connected to a high-sensitivity dc-source unit (HP 4142B), controlled by a computer, and automated I/V as well as lock-in THz response measurements were performed.

In order to be able to derive the current responsivity and NEP values for the GaN transistors, the total THz beam power was measured. This was done using a photo-acoustic Thomas Keating power-meter. The electronic 0.6 THz source yielded a total beam power of $P_{\text{tot}} \sim 450$ μW. For the Picarin lens, a loss factor of 15% is estimated, accounting for the lens material effects as well as aperture truncation of the beam. The power in front of the detector chip amounted to ~ 350 μW. To avoid standing waves appearing between the source and the detector, the beam was further attenuated by 12 dB by placing a set of cardboard sheets into the beam. Hence, the experiment was carried out with a THz beam power of $P_{\text{Beam}} \sim 22$ μW in front of the detector.

TABLE I. DESIGN PARAMETERS AND EXPERIMENTAL DATA OF HEMTS

HEMT Design No.	Gate width W [μm]	Experimentally obtained values		
		V_{Th} [V]	Min. NEP [pW/$\sqrt{\text{Hz}}$]	Max. $\mathfrak{R}_{\text{I}}$ [A/W]
A2	3	-1.7504	125	0.0340
A3	5	-1.9751	155	0.0345
A4	10	-1.7111	190	0.0366
A5	20	-1.7807	490	0.0145
A6	30	-1.7505	870	0.0098
A7	50	-1.7435	1850	0.0049

V. RESULTS AND DISCUSSION

With the setup described in the previous section, the current response characteristics of a set of GaN HEMTs with fixed gate length of 0.25 μm and various gate widths W, as specified in Table I, were recorded. In addition, I/V measurements were carried out for all transistors (data not shown) and the gate-voltage dependencies of the device resistance were extracted from the slopes at zero drain voltage (independently, the resistance curves were also determined from measured current and voltage THz-response curves). The resistance curves were fitted with a sum of two terms, the channel resistance, given by (1), plus a gate-voltage-independent series resistance (with values varying for each transistor) accounting for the ungated channel regions as well as contributions from the transistor contacts. With very satisfactory fits, the series resistance was found to be on the order of 100 Ω (smaller for wider HEMTS). The fits yielded an electron mobility of 970 cm^2/Vs, a non-ideality factor varying from 2.5 to 2.8, and values of the threshold voltage V_{Th} as given in Table I. With these values of V_{Th}, we plot, in Fig. 3, the measured current responses I_{det} of the transistors specified in Table I versus voltage offset $V_{\text{G}} - V_{\text{Th}}$. From each current response curve, the current responsivity of the device was determined by

$$\mathfrak{R}_{\text{I}} = 2.2 \frac{I_{\text{det}}}{P_{\text{Beam}}} \tag{2}$$

unified where the numerical prefactor is a consequence of lock-in detection [18]. The THz signal was amplitude-modulated with a rectangular time signal at 333 Hz. However, the lock-in amplifier used for signal detection, acquires the FET's response to the incident radiation with a sinusoidal time signal, i.e., the peak-to-peak rms value of the first component of a Fourier transform of the rectangular modulation signal, yielding the numerical value of $\pi/\sqrt{2} \approx 2.2$. The maximum responsivity values for each detector are listed in Table I and shown in the inset of Fig. 3. The responsivity as a function of the gate width exhibits a maximum. This is expected to occur for optimal impedance matching. Surprisingly, however, the maximum is found already at a gate width of 10 μm, although simulations suggest a significantly larger gate width and a less pronounced roll-off. This discrepancy might originate from a more complex field distribution at the antenna apex (transition to the HEMT terminals) than assumed.

At this point, we would like to come back to the absolute values of the responsivity, and emphasize that they are conservative estimates, considering that the total available beam power was used for the calculation with (2).

With the obtained responsivity values, the NEP values of the detectors can be determined by

$$\mathrm{NEP} = \frac{\sqrt{4k_\mathrm{B}T}}{\mathfrak{R}_\mathrm{I}\sqrt{R_\mathrm{d}}} \tag{3}$$

This formula assumes only thermal noise contributions which is valid because we work without drain bias, and the gate leakage was found to be negligible close to threshold. A plot of the resulting gate-voltage-dependent NEP values of the detectors is depicted in Fig. 4 and extracted minimum NEP values are listed in Table I. The best device is the narrowest. Although its responsivity is not the highest, this is over-compensated in (3) by the larger channel resistance R_d. Considering the absolute NEP values, note that these values reflect the device sensitivity with respect to the total available THz beam power, neglecting the radiation coupling efficiency into the FET channels. No correction was made for the directional antenna gain. Thus, the responsivity values represent lower bounds and the NEP values upper bounds.

The performance data of the GaN-based THz detectors presented in this contribution compare well with those of CMOS devices of the (nominally) same gate length. For Si MOSFETs with 0.25-μm-long and 0.8-μm-wide channels, we have previously measured NEP values of about 200 pW/$\sqrt{\mathrm{Hz}}$ [19]. Simulations of the performance of these MOSFETs yield a theoretical NEP value of 60 pW/$\sqrt{\mathrm{Hz}}$ [20]. As a consequence, the performances of MOSFETs and GaN HEMTS - as measured by us - are found to be roughly comparable at 0.6 THz. GaN HEMTs may have the potential to become superior, especially if the channel length is reduced. The reasons are as follows: (i) GaN HEMTs - with their higher electron mobility - operate close to the full-plasmonic regime [11] where mixing is more efficient than in the distributed resistive-mixing regime; (ii) the lower channel resistance of the GaN HEMTs facilitates impedance matching with the antenna, even for broad-band (typically low-impedance) antennas.

ACKNOWLEDGMENT

Funding has been provided by the Deutsche Forschungsgemeinschaft (DFG) under contract no. LI 1280/3-1.

REFERENCES

[1] M. Dyakonov and M. Shur, "Detection, mixing, and frequency multiplication of terahertz radiation by two-dimensional electronic fluid," *IEEE Transactions on Electron Devices*, vol. 43, no. 3, pp. 380–387, Mar. 1996.

[2] R. Tauk *et al.*, "Plasma wave detection of terahertz radiation by silicon field effects transistors: Responsivity and noise equivalent power," *Applied Physics Letters*, vol. 89, no. 25, p. 253511, Dec. 2006.

[3] S. Boppel, A. Lisauskas, and H. G. Roskos, "Terahertz array imagers: towards the implementation of terahertz cameras with plasma-wave-based silicon MOSFET detectors," in *Handbook of terahertz technology for imaging, sensing and communications*, D. Saeedkia, Ed. Cambridge: Woodhead Publishing Limited, Jan. 2013, pp. 231–271.

[4] M. S. Shur and R. F. Davis, *GaN-Based Materials and Devices: Growth, Fabrication, Characterization and Performance*. Singapore: World Scientific, Oct. 2004.

[5] J. D. Sun, Y. F. Sun, D. M. Wu, Y. Cai, H. Qin, and B. S. Zhang, "High-responsivity, low-noise, room-temperature, self-mixing terahertz detector realized using floating antennas on a GaN-based field-effect transistor," *Applied Physics Letters*, vol. 100, no. 1, p. 013506, Jan. 2012.

[6] J. D. Sun *et al.*, "Probing and modelling the localized self-mixing in a GaN/AlGaN field-effect terahertz detector," *Applied Physics Letters*, vol. 100, no. 17, p. 173513, Apr. 2012.

[7] A. El Fatimy *et al.*, "AlGaN/GaN high electron mobility transistors as a voltage-tunable room temperature terahertz sources," *Journal of Applied Physics*, vol. 107, no. 2, p. 024504, Jan. 2010.

[8] A. El Fatimy *et al.*, "Terahertz detection by GaN/AlGaN transistors," *Electronics Letters*, vol. 42, no. 23, pp. 1342–1344, Nov. 2006.

[9] W. Knap *et al.*, "Nonresonant detection of terahertz radiation in field effect transistors," *Journal of Applied Physics*, vol. 91, no. 11, pp. 9346–9353, Feb. 2002.

[10] A. Lisauskas, U. Pfeiffer, E. Ojefors, P. H. Bolivar, D. Glaab, and H. G. Roskos, "Rational design of high-responsivity detectors of terahertz radiation based on distributed self-mixing in silicon field-effect transistors," *Journal of Applied Physics*, vol. 105, no. 11, p. 114511, Jun. 2009.

[11] S. Boppel *et al.*, "CMOS integrated antenna-coupled field-effect transistors for the detection of radiation from 0.2 to 4.3 THz," *IEEE Transactions on Microwave Theory and Techniques*, vol. 60, no. 12, pp. 3834–3843, Dec. 2012.

[12] M. Sakowicz *et al.*, "Terahertz responsivity of field effect transistors versus their static channel conductivity and loading effects," *Journal of Applied Physics*, vol. 110, no. 5, p. 054512, Sep. 2011.

[13] S. Khandelwal and T. A. Fjeldly, "A physics based compact model of gate capacitance in AlGaN/GaN HEMT devices," in *8th International Caribbean Conference on Devices, Circuits and Systems (ICCDCS)*, Playa del Carmen, Mar. 2012, pp. 1–4.

[14] M. Shur, T. A. Fjeldly, T. Ytterdal, and K. Lee, "Unified MOSFET model," *Solid-state electronics*, vol. 35, no. 12, pp. 1795–1802, Dec. 1992.

[15] S. A. Chevtchenko, F. Brunner, J. Würfl, and G. Tränkle, "Effect of buffer thickness on DC and microwave performance of AlGaN/GaN heterojunction field-effect transistors," *Physica Status Solidi (a)*, vol. 207, no. 6, pp. 1505–1508, feb 2010.

[16] P. Ivo, "AlGaN/GaN HEMTs reliability: Degradation modes and analysis," Ph.D. dissertation, Technische Universiät Berlin, May 2012.

[17] J. Van Rudd and D. M. Mittleman, "Influence of substrate-lens design in terahertz time-domain spectroscopy," *Journal of the Optical Society of America B*, vol. 19, no. 2, pp. 319–329, Feb. 2002.

[18] A. Lisauskas, D. Glaab, H. G. Roskos, E. Oejefors, and U. R. Pfeiffer, "Terahertz imaging with si MOSFET focal-plane arrays," in *Proc. SPIE 7215 Terahertz Technology and Applications II*, San Jose, CA, Feb. 2009, p. 72150J.

[19] "Unpublished data, measured on devices without integrated amplifiers. because the devices were parts of arrays, a reduced beam power (the part impinging onto the pitch area) was assumed. note that the responsivity is hence defined in a somewhat different way than in the present study."

[20] U. R. Pfeiffer and E. Oejefors, "A 600-GHz CMOS focal-plane array for THz imaging," in *34th Solid-State Circuits Conference (ESSCIRC)*, Edinburgh, Sep. 2008, pp. 110–113.